EC
Journals.ASM.org

Biochemical and Kinetic Characterization of the Recombinant ADP-Forming Acetyl Coenzyme A Synthetase from the Amitochondriate Protozoan *Entamoeba histolytica*

Cheryl P. Jones, Cheryl Ingram-Smith

Eukaryotic Pathogens Innovation Center, Department of Genetics and Biochemistry, Clemson University, Clemson, South Carolina, USA

***Entamoeba histolytica*, an amitochondriate protozoan parasite that relies on glycolysis as a key pathway for ATP generation, has developed a unique extended PP_i-dependent glycolytic pathway in which ADP-forming acetyl-coenzyme A (CoA) synthetase (ACD; acetate:CoA ligase [ADP-forming]; EC 6.2.1.13) converts acetyl-CoA to acetate to produce additional ATP and recycle CoA. We characterized the recombinant *E. histolytica* ACD and found that the enzyme is bidirectional, allowing it to potentially play a role in ATP production or in utilization of acetate. In the acetate-forming direction, acetyl-CoA was the preferred substrate and propionyl-CoA was used with lower efficiency. In the acetyl-CoA-forming direction, acetate was the preferred substrate, with a lower efficiency observed with propionate. The enzyme can utilize both ADP/ATP and GDP/GTP in the respective directions of the reaction. ATP and PP_i were found to inhibit the acetate-forming direction of the reaction, with 50% inhibitory concentrations of 0.81 ± 0.17 mM (mean ± standard deviation) and 0.75 ± 0.20 mM, respectively, which are both in the range of their physiological concentrations. ATP and PP_i displayed mixed inhibition versus each of the three substrates, acetyl-CoA, ADP, and phosphate. This is the first example of regulation of ACD enzymatic activity, and possible roles for this regulation are discussed.**

Entamoeba histolytica, a protozoan parasite that causes amoebic dysentery and amoebic liver abscess in humans, is a leading cause of morbidity and mortality due to parasitic disease worldwide, second only to malaria (1). This parasite has a two-stage life cycle, existing as infectious cysts or motile trophozoites that can reside in the anaerobic confines of the human colon and cause disease. After ingestion of cysts and excystation to release trophozoites, asymptomatic infection can occur when trophozoites remain confined to the intestine. However, the parasite can break through the epithelial lining of the intestine and enter the bloodstream, resulting in an invasive infection. Cell lysis, phagocytosis, and trogocytosis all play a role in pathogenicity and contribute sources of nutrients to this metabolically limited parasite (2).

E. histolytica lacks a functional tricarboxylic acid (TCA) cycle and oxidative phosphorylation and consequently relies on substrate-level phosphorylation to provide high-energy compounds. This amitochondriate protozoan utilizes an unusual PP_i-dependent glycolytic pathway (Fig. 1) in which ATP-dependent phosphofructokinase is replaced by PP_i-dependent phosphofructokinase and pyruvate kinase is replaced by a PP_i-dependent pyruvate phosphate dikinase (3–5). The pyruvate end product of glycolysis is converted to acetyl-CoA by pyruvate:ferredoxin oxidoreductase (PFOR) rather than pyruvate dehydrogenase. Acetyl-CoA can then be broken down to ethanol by a bifunctional aldehyde-alcohol dehydrogenase (ADHE) (6) or to acetate by ADP-forming acetyl-CoA synthetase (ACD; acetate:CoA ligase [ADP-forming]; EC 6.2.1.13), as summarized in the following equation: acetyl-CoA + ADP + P_i ⇆ acetate + CoA + ATP.

This extended PP_i-dependent glycolytic pathway increases the ATP output per glucose molecule to 3 when ethanol is produced and to 5 when acetate is the product. ACD was first identified with acetate-forming activity in *E. histolytica* extracts, and the partially purified enzyme was shown to have activity in both directions of the reaction (7). The only other characterized eukaryotic ACD is that from the amitochondriate *Giardia lamblia* (8–10), for which only substantial acetate-forming activity has been detected (10).

Although not widespread, ACD has been identified in all three domains and is postulated in the conversion of acetyl-CoA to acetate. In archaea, ACD was first identified in *Pyrococcus furiosus* (11, 12), a thermophilic anaerobe that ferments carbohydrates and peptides, and it has now been identified in a number of other archaea, including the thermophilic anaerobes *Pyrococcus woesei*, *Desulfurococcus amylolyticus*, *Hyperthermus butylicus*, and *Thermococcus celer* (13, 14), the hyperthermophilic anaerobic sulfate reducer *Archaeoglobus fulgidus* (15), and the halophilic aerobe *Halobacterium saccharovorum* (13, 14). Native ACD has been purified from *P. furiosus* (11, 12) and *Haloarcula marismortui* (16), and recombinant ACDs have been characterized from *P. furiosus* (17), *A. fulgidus* (18), *Methanococcus jannaschii* (18), *H. marismortui* (16), *Pyrobaculum aerophilum* (16), and *Thermococcus kodakarensis* (19).

A similar role for ACD in acetate production has been proposed in bacteria. Most bacteria have a phosphotransacetylase (PTA) and acetate kinase (ACK), which form a predominant pathway for acetate production from acetyl-CoA. ACD from the phototrophic *Chloroflexus aurantiacus* has recently been purified, and the recombinant enzyme was characterized (20). The syntrophs *Pelotomaculum thermopropionicum* (21) and *Syntrophus aciditrophicus* (22) and the propionic acid-producing *Propionibacterium acidipropionici* (23) all lack genes for the PTA-ACK

Received 13 August 2014 **Accepted** 5 October 2014
Published ahead of print 10 October 2014
Address correspondence to Cheryl Ingram-Smith, cheryli@clemson.edu.

doi:10.1128/EC.00192-14

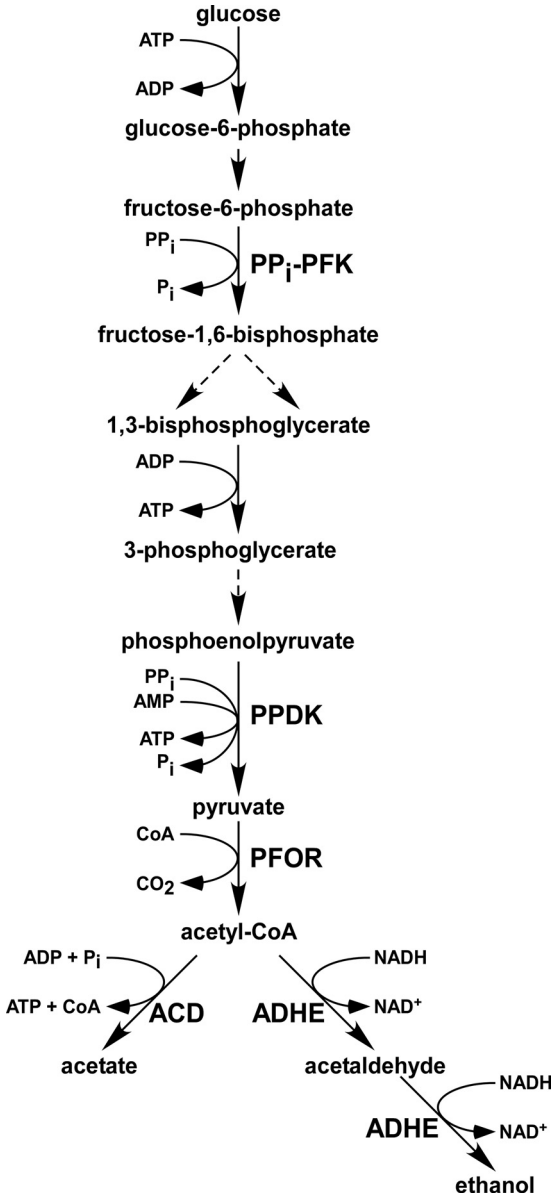

FIG 1 The PP_i-dependent extended glycolytic pathway of *E. histolytica*. Relevant steps that produce or utilize ATP and PP_i are shown, and enzymes that catalyze reactions specific to this pathway are indicated. Dotted arrows represent multiple steps that are not shown. Abbreviations: PP_i-PFK, pyrophosphate-dependent phosphofructokinase; PPDK, pyruvate phosphate dikinase; PFOR, pyruvate:ferredoxin oxidoreductase; ACD, ADP-forming acetyl-CoA synthetase; ADHE, bifunctional aldehyde-alcohol dehydrogenase.

pathway and instead have *acd* genes. ACD has been identified via proteome analysis of *P. acidipropionici* cells grown under acetate-producing conditions, but the enzyme has not been purified or characterized (23). Likewise, the acetate-producing archaea listed above that have ACD lack genes encoding the PTA-ACK pathway.

ACD is part of a superfamily of nucleoside diphosphate-forming acyl-CoA synthetases, which includes the closely related citric acid cycle enzyme succinyl-CoA synthetase (SCS; EC 6.2.1.4) as well as ATP citrate lyase (EC 2.3.3.8) and malate thiokinase (EC 6.3.1.9) (9). SCS has been extensively studied kinetically and structurally (24–26), and a three-step enzymatic mechanism has been proposed (27), with E in the equations representing the enzyme of interest: (i) succinyl-CoA + $P_i \leftrightarrows$ E~succinyl-P + CoA; (ii) E~succinyl-P $\leftrightarrows$ E-His~P + succinate; (iii) E-His~P + ADP $\leftrightarrows$ ATP.

Based on their studies with *P. furiosus* ACD, Brasen et al. (28) proposed that ACD proceeds through a mechanism similar to that of SCS, but with an additional step in which the phosphoryl group is transferred from a His residue on the α-subunit to a His residue on the β-subunit before transfer to ADP in the final step to produce ATP. Here we report the biochemical and kinetic characterizations of the recombinantly produced ACD from the intestinal parasite *E. histolytica* and reveal its ability to function in either acetate production or utilization *in vitro*. Our results confirm that both the acetyl-CoA-forming and acetate-forming activities of ACD are present in cell lysates from *E. histolytica* trophozoites. Inhibition studies suggest *E. histolytica* ACD (EhACD) is regulated through inhibition by ATP and PP_i in the acetate-forming direction.

MATERIALS AND METHODS

Materials. Chemicals were purchased from Sigma-Aldrich, VWR International, Gold Biotechnology, Fisher Scientific, Atlanta Biological, Life Technologies, and JR Scientific.

Growth of *E. histolytica* trophozoites and preparation of cell lysates. *E. histolytica* strain HM-1:IMSS (kindly provided by Lesly Temesvari, Clemson University) was cultured axenically at 37°C in TYI-S-33 medium (29). Cells were harvested by incubation on ice for 10 min and centrifugation at ~350 × *g* for 5 min at 4°C. The pellet was resuspended in 0.8 ml lysis buffer [50 mM Tris-HCl (pH 7.3), 1 mM 4-(2-aminoethyl)benzenesulfonyl fluoride hydrochloride, 0.015 mM E-64, 0.02 mM pepstatin A, 5 mM 1,10-phenanthroline] and disrupted by five cycles of freezing in a dry ice/ethanol bath and thawing at 37°C. The cell lysate was kept on ice, and enzymatic activity was assayed immediately by using the 5,5′-dithio-bis-(2-nitrobenzoic acid) (DTNB) and hydroxamate assays described below. Total protein concentration was determined by using the Bradford method (30) with bovine serum albumin as the standard.

Production and purification of *E. histolytica* ACD. A codon-optimized *E. histolytica acd* gene was synthesized by Genscript and cloned into pET21b (Novagen) for production of recombinant *E. histolytica* ACD in *Escherichia coli*. The pET21b-*ACD* plasmid was transformed into *E. coli* Rosetta2(DE3)pLysS cells (Novagen), and cultures were grown in Luria-Bertani medium (LB) containing 50 μg ml^{-1} ampicillin and 34 μg ml^{-1} chloramphenicol, with shaking at 200 rpm at 37°C to an A_{600} of ~0.8. Protein production was initiated by the addition of isopropyl β-D-1-thiogalactopyranoside (IPTG) to a final concentration of 0.5 mM. Cultures were grown overnight at ambient temperature and harvested by centrifugation. Cells were suspended in ice-cold buffer A (25 mM Tris-HCl, 150 mM NaCl, 10% glycerol, 20 mM imidazole [pH 7.4]) and disrupted by two passages through a French pressure cell at 138 MPa. The cell lysate was clarified via ultracentrifugation at ~ 98,000 × *g* for 1 h at 4°C, and cell extract was applied to a 5-ml HisTrap HP nickel affinity column (GE Healthcare) equilibrated with buffer A. After extensive washing with buffer A to remove unbound protein, the column was developed with a linear gradient of 0 to 0.5 M imidazole in buffer A. Fractions containing active enzyme were pooled, dialyzed overnight in buffer (25 mM Tris-HCl, 10% glycerol [pH 7.0]), aliquoted, and stored at −80°C. The enzyme was judged to be electrophoretically pure by SDS-PAGE analysis. Protein concentrations were determined based on the absorbance at 280 nm using a Take3 microvolume plate (BioTek).

Determination of molecular mass. The native molecular mass of EhACD was determined by gel filtration chromatography through a Superose 12 column (GE Healthcare) preequilibrated with 50 mM Tris-HCl, 150 mM NaCl (pH 7.0). The column was calibrated with cytochrome *c* (12.4 kDa), carbonic anhydrase (29 kDa), albumin (66 kDa), amylase (200

kDa), apoferritin (443 kDa), and thyroglobulin (669 kDa) and developed at a flow rate of 0.5 ml per minute.

Determination of kinetic parameters for EhACD. Pseudo-first-order reaction kinetic determinations were performed in both directions of the reaction. Enzymatic activity in the acetate-forming direction was determined by measuring the release of CoA with a sulfhydryl group (CoASH) from acyl-CoA by using Ellman's thiol reagent (DTNB) (31). Production of NTB^{2-} by CoASH cleavage of DTNB was measured spectrophotometrically at 412 nm. Reaction mixtures (50 mM Tris-HCl, 0.3 mM DTNB, 6 mM HEPES [used to solubilize DTNB] [pH 7.3]) with varied substrate concentrations were preincubated at 37°C for 5.5 min. Assays were performed in 96-well plates in 0.2-ml reaction volumes. Reactions were initiated by the addition of enzyme, and absorbance was measured every 4 s at 37°C by using a Synergy HT multimode microplate reader (BioTek). Initial velocities were converted to micromoles of CoASH formed by using an extinction coefficient (ε) of 13.6 mM^{-1} cm^{-1} for the thiophenolate NTB^{2-} anion. One unit of activity was defined as 1 micromole of product per minute per milligram of protein. In determinations of kinetic parameters for acetate formation, nonvaried substrate concentrations were held at 0.3 mM acetyl-CoA, 8 mM KH_2PO_4, and 5 mM $MgCl_2$:ADP or 6 mM $MgCl_2$:GDP. For propionate formation, nonvaried substrate concentrations were held at 0.3 mM propionyl-CoA, 12.5 mM KH_2PO_4, and 3 mM $MgCl_2$:ADP.

Activity in the acetate-forming direction was confirmed using the hexokinase/glucose-6-phosphate dehydrogenase-coupled assay (32). This assay couples ATP formation to the reduction of $NADP^+$ to NADPH, which is measured spectrophotometrically at 340 nm. Reaction mixtures (100 mM Tris-HCl [pH 7.3], 5.5 mM glucose, 1 mM $NADP^+$, 0.2 mM dithiothreitol) with varied concentrations of substrates were preincubated at 37°C for 5.5 min, hexokinase and glucose-6-phosphate dehydrogenase were added, and the reactions were initiated by the addition of ACD. Assays were performed in 96-well plates in 0.2-ml reaction volumes, and absorbance was measured every 4 s at 37°C by using a Synergy HT multimode microplate reader (BioTek). Initial velocities were converted to micromoles of ATP formed by using an extinction coefficient of 6.22 mM^{-1} cm^{-1} for NADPH. Concentrations of nonvaried substrates used for both the DTNB assay and coupled enzyme assay were identical.

Enzymatic activity for determination of acetyl-CoA formation was detected using the hydroxamate assay (33, 34). Reaction mixtures (50 mM Tris-HCl [pH 7.5], 300 mM hydroxylamine-HCl [pH 7.0]) with varied substrate concentrations were preincubated at 37°C for 5.5 min, and reactions were initiated by the addition of enzyme. Reactions (0.15-ml reaction volumes) were terminated by the addition of 1 volume of stop solution (2.5% $FeCl_3$, 2 N HCl, 10% trichloroacetic acid), and the absorbance at 540 nm was measured. Product formation was determined by comparison to an acetyl-CoA standard curve. For acyl substrates prepared in ethanol, the final concentration of ethanol in the reaction mixture was kept at 2.5%, which was determined not to affect enzymatic activity. One unit of activity was defined as 1 micromole of acetyl-CoA produced per minute per milligram of protein. In determinations of kinetic parameters for acetyl-CoA formation, the nonvaried substrates were held at 100 mM acetate, 1 mM CoA, 20 mM $MgCl_2$:ATP, and 25 mM $MgCl_2$:GTP. For determination of kinetic parameters for propionyl-CoA formation, the nonvaried substrates were held at the following concentrations: 250 mM propionate, 3 mM CoA, and 20 mM $MgCl_2$:ATP.

Apparent kinetic parameters were determined by varying the concentration of a single substrate while the concentrations of the other two substrates were held constant. For determination of the apparent steady-state kinetic parameters K_m, k_{cat}, and k_{cat}/K_m, and their standard deviations (SD), nonlinear regression in KaleidaGraph (Synergy Software) was used to fit the data to the Michaelis-Menten equation.

Determination of inhibition parameters. Various metabolic intermediates were tested as effectors of ACD. The IC_{50}s (the effector concentrations that provided half-maximal inhibition) for inhibitors were determined based on K_m substrate concentrations by measuring the decrease in enzymatic activity as a function of increasing concentration of inhibitor. Nonlinear regression analysis in Prism 5 (GraphPad Software) was used to fit the data to the log [inhibitor] versus response curve to determine IC_{50}s. To examine the mode of inhibition, enzymatic activity was assayed in each direction in a four-by-four matrix of varied inhibitor concentrations versus varied concentrations of one substrate, with the other two substrate concentrations held constant. Linear regression in KaleidaGraph (Synergy Software) was used to resolve the points of intersection of the inverse plots.

RESULTS

General characterization. The limited characterization of partially purified native *E. histolytica* ACD reported by Reeves et al. (7) indicated that the enzyme has a narrow nucleotide specificity. To allow a more thorough characterization of the *E. histolytica* ACD (EhACD), we produced the recombinant enzyme in *E. coli*. A codon-optimized gene was synthesized by Genscript and cloned into the pET21b *E. coli* expression vector (Novagen), which encodes the addition of a C-terminal His_6 tag to the recombinant protein. The calculated subunit molecular mass of the recombinant His-tagged protein was 78,999 Da. The molecular mass of the purified enzyme was estimated to be ~150 kDa based on gel filtration chromatography, suggesting that EhACD is dimeric, as found with the *G. lamblia* ACD (10). The optimum temperature for ACD activity was determined to be 55°C in the acetyl-CoA-forming direction but could not be determined in the acetate-forming direction due to limitations of the equipment used for measurements. This unexpectedly high optimal temperature may have been an artifact from the assay conditions or may represent an unusual stability of this protein, but it was not analyzed further. However, activity was routinely assayed at 37°C, the temperature *E. histolytica* trophozoites would typically encounter within the human host. The enzyme had approximately 70% activity at this temperature versus its optimum temperature.

The requirement for a divalent cation was examined and ACD was found to have the highest activity with Mg^{2+} and Mn^{2+} and substantial activity with Co^{2+} in both directions of the reaction, but only weak activity with Ni^{2+}, Zn^{2+}, Ca^{2+}, and Cu^{2+} (Fig. 2). The preference for Mg^{2+}, Mn^{2+}, and Co^{2+} is similar to that of other ACDs (10, 11, 18).

ACD enzymatic activity was observed in both directions of the reaction, and the reaction rate was linearly dependent on enzyme concentration. Specific activity in the acetate-forming direction (85 ± 1.2 μmol min^{-1} mg^{-1}) was approximately half that observed in the acetyl-CoA-forming direction (180 ± 2.0 μmol min^{-1} mg^{-1}). Similarly, measurement of ACD specific activity in *E. histolytica* cell extracts showed that activity in the acetate-forming direction was approximately half that in the acetyl-CoA-forming direction (0.14 ± 0.022 μmol min^{-1} mg^{-1} versus 0.29 ± 0.004 μmol min^{-1} mg^{-1}). In contrast, ACD activity in *Giardia* cell extracts could only be detected in the direction of acetate formation (10). Although the purified recombinant *Giardia* ACD had activity in both directions of the reaction, the acetyl-CoA-forming activity was ~4% of the acetate-forming activity (9).

EhACD has a limited acyl-CoA substrate range, with the highest activity observed with acetyl-CoA and lower activity observed with propionyl-CoA (16% ± 2.8% activity versus that with acetyl-CoA). Less than 1% activity was observed with isobutyryl-CoA and isovaleryl-CoA at a 0.3 mM final concentration, and no activity was observed with butyryl-CoA, succinyl-CoA, or phenylacetyl-CoA. ADP and GDP gave the highest activity (100% ± 1.0%

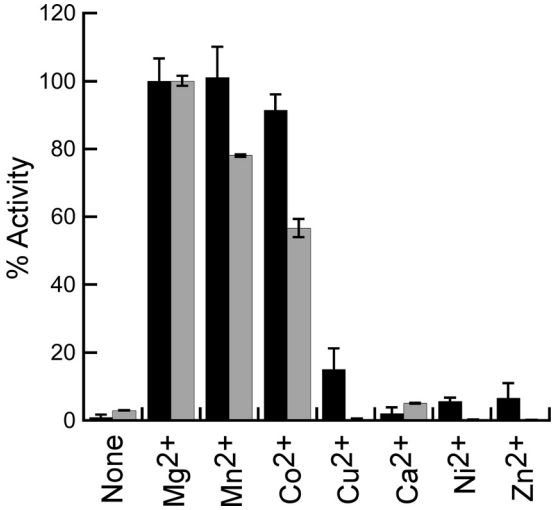

FIG 2 Divalent cation specificity of EhACD. Activities were determined in each direction of the reaction by using saturating substrate conditions in the presence or absence of metals (3 mM final concentration in the acetate-forming direction and 20 mM final concentration in the acetyl-CoA forming direction). Activities were normalized to the activity observed with Mg^{2+}. White bars, activities in the acetate-forming direction; gray bars, activities in the acetyl-CoA-forming direction. Reported activities are means ± SD of three replicates.

and 106% ± 3.7% activity, respectively), although activity was also observed with IDP (28% ± 3.8%), CDP (7.0% ± 0.2%), and UDP (2.8% ± 0.1%); no activity was observed with TDP as the substrate. PP_i was tested with AMP as the phosphoryl acceptor, but no activity was observed under the conditions tested.

In the acyl-CoA-forming direction, acetate was the favored substrate and propionate and butyrate could also be used, with relative activities of 72% ± 1.5% and 5.6% ± 0.2%, respectively, versus acetate. Less than 4% activity was observed with isobutyrate, valerate, isovalerate, hexanoate, heptanoate, octanoate, succinate, or phenylacetate as the acyl substrate. Activity observed with ATP (representing 100% activity) was nearly double that with GTP (57% ± 0.4%) and substantially higher than the activities observed with ITP (15% ± 0.2%), CTP (4.1% ± 0.3%), or UTP (1.6% ± 0.2%); no activity was observed with TTP or PP_i.

Kinetic parameters. Kinetic parameters for EhACD were determined in both the acetate-forming and acetyl-CoA-forming directions (Table 1). Activity decreased at substrate concentrations above 6 mM ADP or 25 mM ATP in the respective directions of the reaction, so the concentrations of these substrates were held below saturation in determinations of kinetic parameters. Under these conditions, acetyl-CoA and P_i in the acetate/ATP-forming direction and acetate and CoA in the acetyl-CoA-forming direction followed Michaelis-Menten-like kinetics. The enzyme displayed similar K_m values for acetyl-CoA and propionyl-CoA in the acetate-forming direction of the reaction. However, the turnover rate, k_{cat}, was approximately 5-fold higher with acetyl-CoA versus propionyl-CoA, resulting in ~4-fold-higher catalytic efficiency with acetyl-CoA. The K_m for P_i was similar with acetyl-CoA or propionyl-CoA as the acyl substrate, but the K_m for ADP was reduced ~2-fold with propionyl-CoA versus acetyl-CoA. Similar K_m and k_{cat} values were observed with ADP and GDP (Table 1). The K_m values observed for EhACD are similar to those reported for the *Giardia* ACD (0.02 mM, 0.23 mM, and 1.59 mM for acetyl-CoA, ADP, and P_i, respectively) (10).

As the enzyme assay used for determination of kinetic parameters in the acetate-forming direction of the reaction measures the CoA release in the first step, we confirmed our results by using a coupled enzyme assay that measures ATP production in the last step of the reaction. Similar K_m and k_{cat} values were observed with this assay (acetyl-CoA, 0.017 ± 0.001 mM [K_m] and 130 ± 14 s^{-1} [k_{cat}]; KH_2PO_4, 2.1 ± 0.21 mM and 180 ± 16 s^{-1}; ADP, 0.94 ± 0.16 mM and 140 ± 7.2 s^{-1}).

In the acetyl-CoA-forming direction of the reaction, the K_m for acetate was ~2-fold higher than that for propionate (Table 1); however, the k_{cat} values were similar for both substrates, unlike in the opposite direction. Thus, the catalytic efficiency of EhACD with acetate was only 2.6-fold higher than with propionate. The K_m for CoA was ~2-fold elevated with propionate versus acetate as the acyl substrate, but the K_m for ATP was slightly reduced. The K_m values for ATP and GTP were similar, but the turnover rate was reduced 1.8-fold with GTP. The overall catalytic efficiency with ATP was only 1.5-fold higher than with GTP, indicating that both are suitable substrates. Although weak activity was observed with butyrate, kinetic parameters could not be determined, as the enzyme was unsaturable for butyrate even at concentrations as high as 1 M.

Enzyme inhibition. Since ACD can function to produce either ATP or acetyl-CoA, regulation of this enzyme may be important for maintaining proper levels of these metabolites in the cell. An array of metabolic intermediates was tested as effectors for ACD (Fig. 3). ATP and PP_i were found to be potent inhibitors in the acetate-forming direction of the reaction, producing greater than 95% inhibition at a 10 mM final concentration (Fig. 3). Additionally, 50% or less activity was observed in the presence of 10 mM glyoxylate (32% ± 2%), NAD^+ (47% ± 3%), or glucose-6-phosphate (50% ± 5%). In the acetyl-CoA-forming direction, only weak to moderate inhibition was observed with any of the com-

TABLE 1 Apparent kinetic parameters for EhACD in each direction of the reaction[a]

Reaction direction and varied substrate	K_m (mM)	k_{cat} (s^{-1})	k_{cat}/K_m (s^{-1} mM^{-1})
Acetate-forming direction			
Acetyl-CoA	0.04 ± 0.001	110 ± 1.6	2,600 ± 370
Phosphate	1.8 ± 0.18	120 ± 7.8	65 ± 2.3
ADP	1.6 ± 0.15	140 ± 1.2	89 ± 7.9
GDP	1.9 ± 0.14	170 ± 5.2	90 ± 8.3
Propionyl-CoA	0.032 ± 0.002	21 ± 0.6	650 ± 63
Phosphate	1.5 ± 0.09	18 ± 0.6	12 ± 0.5
ADP	0.71 ± 0.09	24 ± 0.3	34 ± 3.4
Acetyl-CoA-forming direction			
Acetate	14 ± 0.6	240 ± 2.7	16 ± 0.5
CoA	0.20 ± 0.01	220 ± 4.3	1,100 ± 57
ATP	12 ± 0.4	320 ± 4.4	27 ± 0.7
GTP	10 ± 0.1	180 ± 1.6	18 ± 0.1
Propionate	29 ± 1.4	190 ± 1.5	6.3 ± 0.3
CoA	1.6 ± 0.05	260 ± 2.0	160 ± 4.3
ATP	7.2 ± 0.7	240 ± 7.1	33 ± 2.2

[a] Values are means ± SD.

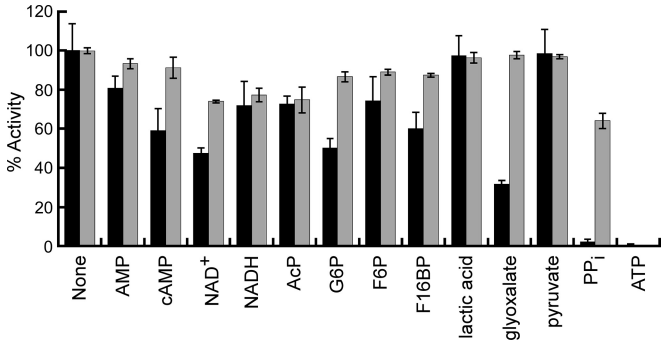

FIG 3 Effects of various metabolites on EhACD activity. Activities were determined in each direction of the reaction by using K_m concentrations of substrate in the presence or absence of the indicated metabolites at a final concentration of 10 mM. Note that ATP was tested only in the acetate-forming direction, since it serves as a substrate in the acetyl-CoA-forming direction. Activities were normalized to the activity observed in the absence of added metabolites. Black bars, activities in the acetate-forming direction; gray bars, activities in the acetyl-CoA-forming direction. Reported activities are means ± SD of three replicates. Abbreviations: cAMP, cyclic AMP; AcP, acetyl phosphate; G6P, glucose 6-phosphate; F6P, fructose 6-phosphate; F16BP, fructose 1,6-bisphosphate.

pounds tested (Fig. 3). PP_i had only a moderate effect in this direction, reducing activity to 64% ± 4% when present at a 10 mM final concentration in the reaction mixture. ATP is a substrate in this direction, and although it does inhibit at higher concentrations, we did not examine this further.

In addition to the intermediates shown in Fig. 3, glyceraldehyde-3-phosphate, phosphoenolpyruvate, and oxaloacetate were tested, but only in the acetyl-CoA-forming direction, because they interfere with the assays used for the acetate-forming direction. None of these compounds resulted in any substantial inhibition in this direction, with 85% ± 0.3%, 85% ± 5.1%, and 90% ± 1.4% activity observed, respectively.

IC_{50}s for ATP and PP_i in the acetate-forming direction were determined to be 0.81 ± 0.17 mM for ATP and 0.83 ± 0.27 mM for PP_i. The estimated intracellular concentrations of ATP and PP_i in *E. histolytica* trophozoites grown in the presence of glucose are 5 ± 2 mM and 0.45 mM, respectively (35), suggesting that regulation of the acetate-forming activity of ACD by ATP and PP_i is biologically relevant. The mode of inhibition by each of these compounds was determined by kinetic analysis in which the concentration of inhibitor was varied versus one substrate and the concentrations of the other two substrates were held constant. These analyses suggested mixed inhibition by ATP (Fig. 4) and PP_i (Fig. 5) versus each substrate.

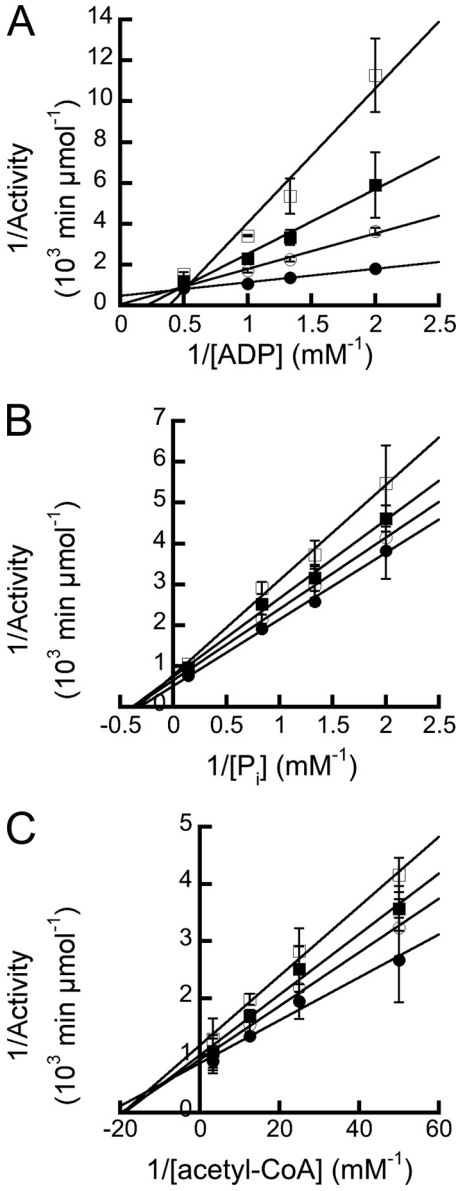

FIG 4 The inhibitory effects of ATP versus ADP, acetyl-CoA, and phosphate in the acetate-forming direction. Activity was determined in the presence of various ATP concentrations, with the concentration of one substrate varied and the others held constant. ATP concentrations used were 0 mM (●), 0.2 mM (○), 0.35 mM (■), and 0.5 mM (□). ATP inhibition patterns were observed versus ADP (A), acetyl-CoA (B), and KH_2PO_4 (C). Reported activities are means ± SD of three replicates.

DISCUSSION

Substrate specificity of EhACD and comparison to other characterized ACDs. Although ACD is not widespread, characterization of *P. furiosus* ACDs has demonstrated that there are at least two different isoforms (11, 12). This was confirmed by characterization of additional enzymes from *A. fulgidus* (18) and *T. kodakarensis* (19). The ACD I isoforms prefer acetate and acetyl-CoA and can typically utilize propionate, butyrate, and propionyl-CoA as well but do not tend to use longer or branched-chain acyl/acyl-CoA derivatives (11, 12, 16, 18, 20). The ACD II isoforms prefer longer acyl/acyl-CoA derivatives, such as phenylacetyl-CoA/phenylacetate and indoleacetate as the substrates (12, 18, 19). Based on our characterization of recombinant EhACD and the previous characterization of the partially purified native EhACD (7), this enzyme belongs to the ACD I class. The *Giardia* enzyme also appears to belong to this class (10).

All ACDs utilize ADP, but the ability to accept GDP as a substrate varies (11, 12, 16). In contrast to SCS, which has an isozyme specific for each (24), and the *G. lamblia* ACD, which functions only with ADP (10), EhACD is able to utilize ADP and GDP interchangeably, with similar K_m and k_{cat} values for each. However, EhACD may be more likely to utilize ADP *in vivo*, since the estimated intracellular concentration of ADP is higher than that for

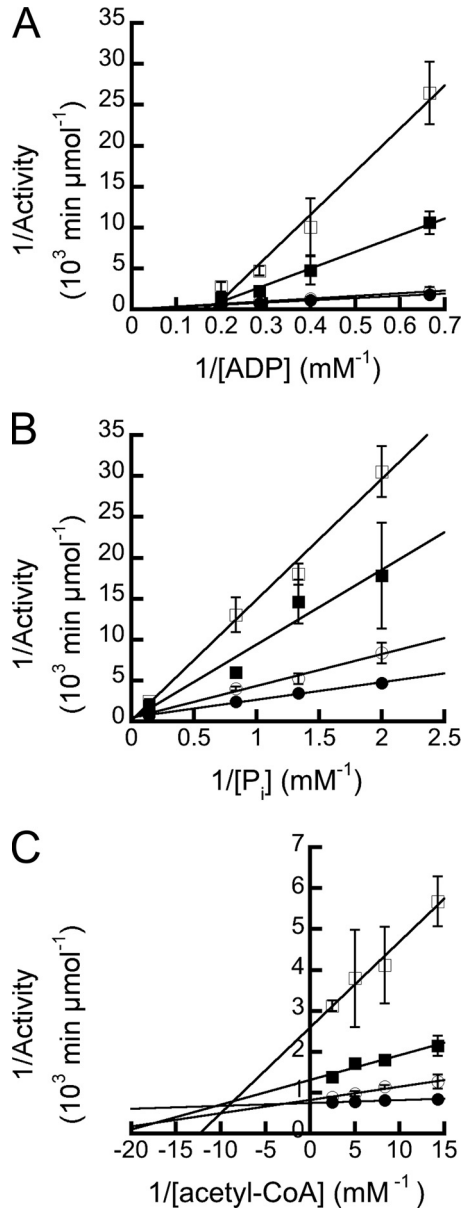

FIG 5 The inhibitory effects of PP_i on ADP, acetyl-CoA, and phosphate in the acetate-forming direction. Activity was determined in the presence of various PP_i concentrations, with the concentration of one substrate varied and the others held constant. PP_i concentrations used were 0.6 mM (●), 2 mM (○), 3.5 mM (■), and 6 mM (□). PP_i inhibition patterns were observed versus ADP (A), acetyl-CoA (B), and KH_2PO_4 (C). Reported activities are means ± SD of three replicates.

GDP (3.3 ± 1.2 mM versus 0.7 mM, respectively [35]). Furthermore, the intracellular concentration for ADP is above the K_m value for ADP, whereas the intracellular GDP concentration is below the K_m value. Like EhACD, *Entamoeba* phosphoglycerate kinase can use both ADP and GDP but shows a strong preference for GDP, as judged by the order-of-magnitude difference between the K_m values for these substrates (4).

In the acetyl-CoA-forming direction of the reaction, the enzyme does not show a clear preference for ATP or GTP, as the kinetic parameters with each substrate are similar. The fact that the intracellular concentrations of ATP and GTP (5 ± 2 mM and 1.8 mM, respectively [35]) are both below the K_m values for these substrates suggests that the acetate/ATP-forming direction of the reaction is favored in the cell, even though the purified enzyme has similar activity in both directions. The higher catalytic efficiency observed with either substrate in the acetate-forming direction versus the acetyl-CoA-forming direction is consistent with this.

A comparison of the characterized ACD I enzymes reveals a great deal of variability. All of the characterized enzymes catalyzed the acetate/ATP-forming reaction, but an acetyl-CoA-forming activity was not detected or was very low for the ACDs from *G. lamblia* (8–10), *P. aerophilum* (16), and *M. jannaschii* (18). A range of K_m values has been observed for each substrate in both directions of the reaction (Table 2). Within the archaea, for which six ACD I enzymes have been characterized, the K_m for a given substrate in the acetyl-CoA-forming direction showed up to an 11-fold range in values. In the acetate/ATP-forming direction, K_m values ranged up to 41-fold for acetyl-CoA. The K_m values observed for the single characterized bacterial ACD, from *C. aurantiacus*, were within the range of values observed with the archaeal enzymes. Likewise, the K_m values observed for the *G. lamblia* enzyme were within or near the ranges of those for the archaeal enzymes.

For EhACD, the K_m values for acetyl-CoA and P_i were comparable to those for other enzymes, but the K_m for ADP was substantially higher. In the acetyl-CoA-forming direction, the K_m value for CoA was slightly above the range observed for other ACDs. However, the K_m for acetate was 8-fold higher than the highest K_m observed for any other ACD, and the K_m for ATP was over 20-fold higher. This may suggest that acetyl-CoA formation is not the preferred direction of the reaction and that *E. histolytica* may employ this direction only under specific environmental or physiological conditions (see below).

Role of the extended glycolytic pathway. The PP_i-dependent extended glycolytic pathway branches after production of acetyl-CoA from pyruvate. In one branch, ACD is responsible for production of acetate and ATP; in the other, acetyl-CoA is metabolized to ethanol by ADHE (6). Montalvo et al. (36) and Reeves et al. (7) showed that ethanol and acetate are produced at approximately a 2:1 ratio under anaerobic conditions versus a 1:2 ratio under aerobic conditions. More recently, Pineda et al. (37) found

TABLE 2 Comparison of K_m values for characterized ACD I enzymes

Substrate	K_m (µM)			
	Archaeal ACDs (range)	Bacterial ACD[f]	*Giardia* ACD[g]	EhACD
Acetyl-CoA	10[a] to 410[b]	37	20	40
Phosphate	100[d] to 1,300[b,c]	1,000	1,590	1,800
ADP	7[a] to 150[d]	91	230	1,600
Acetate	340[a] to 1,700[b]	900	ND[h]	14,000
CoA	5.6[e] to 60[b]	24	ND	200
ATP	56[e] to 477[d]	570	ND	12,000

[a] Reported K_m for *Archaeoglobus fulgidus* (18).
[b] Reported K_m for *Haloarcula marismortui* (16).
[c] Reported K_m for *Pyrobaculum aerophilum* (16).
[d] Reported K_m for *Pyrococcus furiosus* (12).
[e] Reported K_m for *Thermococcus kodakarensis* (19).
[f] Reported K_m for *Chloroflexus aurantiacus* (20).
[g] Reported K_m for *Giardia lamblia* (10).
[h] ND, no activity detected in the direction of acetyl-CoA formation.

an ethanol-to-acetate ratio of 3.9:1 was produced in cells growing under standard conditions. Upon exposure to oxygen-saturated medium, however, the flux through acetate increased for up to 90 min. The flux through ethanol decreased but gradually recovered over time. Overall, these results suggest ethanol and acetate are both important end products of glycolysis and that flux through both of these pathways may be necessary to generate sufficient ATP while still providing for NAD^+ recycling.

ACD may also play a role in ATP production from amino acid catabolism. In addition to increasing ATP production from glycolysis, the presence of ACD and PFOR allows certain amino acids to be catabolized for ATP production. *E. histolytica* trophozoites scavenge a number of amino acids. Asparagine, aspartate, and tryptophan are broken down to pyruvate, and methionine, threonine, and homocysteine are broken down to 2-oxobutanoate (38). PFOR converts these products, respectively, to acetyl-CoA and propionyl-CoA (7, 39, 40), which can then serve as the substrates of ACD for ATP production.

Regulation of ACD activity. Although metabolic flux analysis using kinetic modeling suggested that ACD has little regulatory effect over glycolysis (35), its roles in amino acid degradation were not taken into account. On the contrary, one might expect that ACD's position in the extended glycolytic pathway of *E. histolytica* makes it a prime site for regulation in order to properly maintain ATP and acetyl-CoA concentrations. In fact, we have found that EhACD is regulated by both ATP and PP_i in the acetate-forming direction, with IC_{50}s that are within the physiological range based on the estimated intracellular concentrations for each (35). An excess of ATP would indicate that the energy needs of the cell are being met, and thus additional ATP production by ACD would be unnecessary. This would prevent costly depletion of acetyl-CoA, which could instead be used by other pathways.

PP_i serves as a phosphoryl donor for two PP_i-dependent glycolytic enzymes in *E. histolytica* (4). A buildup of PP_i may signal a backup in glycolysis, which would also warrant inhibition of ACD to prevent depletion of acetyl-CoA. Finally, regulation of ACD by two components of the glycolytic pathway may provide a means for shunting acetyl-CoA to ADHE for ethanol production to regenerate NAD^+, thus maintaining a proper balance between these two alternative pathways.

Differences between *G. lamblia* and *E. histolytica* allow these microorganisms to occupy diverse habitats. Although *E. histolytica* and *G. lamblia* rely on similar extended PP_i-dependent glycolytic pathways, the *E. histolytica* ACD is able to function in both the acetate-forming and acetyl-CoA-forming directions of the reaction, whereas the *Giardia* enzyme is limited to just the acetate-forming direction (10). This divergence may have arisen due to the different environments these parasites inhabit during infection. *Entamoeba* trophozoites reside in the mucus layer of the colon, where bacterial microflora produce large amounts of the short-chain fatty acids (SCFA) acetate, propionate, and butyrate (41). *Giardia* colonizes the small intestine, in which the SCFA concentration is relatively low (41), and thus it is unlikely that ACD is needed in acetate utilization.

The total SCFA concentration in the human colon is approximately 100 to 120 mM, with relative molar ratios of 57:22:21 (acetate:propionate:butyrate) (41), giving approximate concentrations of 57 to 68 mM for acetate, 22 to 26 mM for propionate, and 21 to 25 mM for butyrate. Acetate and propionate concentrations are thus in a range that would suggest ACD's activity in the acetyl-CoA-forming direction may be physiologically relevant and that ACD may switch from acetate/ATP production when glucose is present to SCFA utilization when glucose becomes limiting.

Concluding remarks. Although we have speculated on the roles of ACD in *Entamoeba*, experimental confirmation is still required. In addition to *Entamoeba* and *Giardia*, ACD may also be present in other parasites, including *Cryptosporidium muris*, *Blastocystis hominis*, and *Plasmodium falciparum*. The possible existence of ACD in *Plasmodium* is of particular interest, not only because of its enormous public health significance but also because the parasites retain fully functional mitochondria. Within the complex life cycle of *Plasmodium*, the intraerythrocyte stages rely primarily on the incomplete oxidation of blood glucose by glycolysis to produce ATP (42, 43), and thus ACD may play a similar role as in *Entamoeba*. Whether ACD plays similar roles in other parasites must still be investigated, and results from such studies may provide insights into energy metabolism in these important eukaryotic pathogens.

ACKNOWLEDGMENTS

We gratefully acknowledge Kerry Smith (Clemson University) for helpful discussions on this research and comments on the preparation of the manuscript.

Support for this research was provided by National Science Foundation Award 0920274 (Kerry Smith, PI, and Cheryl Ingram-Smith, co-I), a National Science Foundation Graduate Research Fellowship award to C.J., and Clemson University.

REFERENCES

1. **World Health Organization.** 1997. Amoebiasis. Wkly. Epidemiol. Rec. **72:**97–100.
2. **Marie C, Petri WA, Jr.** 2014. Regulation of virulence of *Entamoeba histolytica*. Annu. Rev. Microbiol. **68:**493–520. http://dx.doi.org/10.1146/annurev-micro-091313-103550.
3. **Reeves RE, Serrano R, South DJ.** 1976. 6-Phosphofructokinase (pyrophosphate): properties of the enzyme from *Entamoeba histolytica* and its reaction mechanism. J. Biol. Chem. **251:**2958–2962.
4. **Saavedra E, Encalada R, Pineda E, Jasso-Chavez R, Moreno-Sanchez R.** 2005. Glycolysis in *Entamoeba histolytica*: biochemical characterization of recombinant glycolytic enzymes and flux control analysis. FEBS J. **272:**1767–1783. http://dx.doi.org/10.1111/j.1742-4658.2005.04610.x.
5. **Saavedra-Lira E, Perez-Montfort R.** 1996. Energy production in *Entamoeba histolytica*: new perspectives in rational drug design. Arch. Med. Res. **27:**257–264.
6. **Lo HS, Reeves RE.** 1978. Pyruvate-to-ethanol pathway in *Entamoeba histolytica*. Biochem. J. **171:**225–230.
7. **Reeves RE, Warren LG, Susskind B, Lo HS.** 1977. An energy-conserving pyruvate-to-acetate pathway in *Entamoeba histolytica*: pyruvate synthase and a new acetate thiokinase. J. Biol. Chem. **252:**726–731.
8. **Lindmark DG.** 1980. Energy metabolism of the anaerobic protozoon *Giardia lamblia*. Mol. Biochem. Parasitol. **1:**1–12. http://dx.doi.org/10.1016/0166-6851(80)90037-7.
9. **Sanchez LB, Galperin MY, Muller M.** 2000. Acetyl-CoA synthetase from the amitochondriate eukaryote *Giardia lamblia* belongs to the newly recognized superfamily of acyl-CoA synthetases (nucleoside diphosphate-forming). J. Biol. Chem. **275:**5794–5803. http://dx.doi.org/10.1074/jbc.275.8.5794.
10. **Sanchez LB, Muller M.** 1996. Purification and characterization of the acetate forming enzyme, acetyl-CoA synthetase (ADP-forming) from the amitochondriate protist, *Giardia lamblia*. FEBS Lett. **378:**240–244. http://dx.doi.org/10.1016/0014-5793(95)01463-2.
11. **Glasemacher J, Bock AK, Schmid R, Schonheit P.** 1997. Purification and properties of acetyl-CoA synthetase (ADP-forming), an archaeal enzyme of acetate formation and ATP synthesis, from the hyperthermophile *Pyrococcus furiosus*. Eur. J. Biochem. **244:**561–567. http://dx.doi.org/10.1111/j.1432-1033.1997.00561.x.
12. **Mai X, Adams MW.** 1996. Purification and characterization of two reversible

and ADP-dependent acetyl coenzyme A synthetases from the hyperthermophilic archaeon *Pyrococcus furiosus*. J. Bacteriol. **178:**5897–5903.
13. **Schafer T, Schonheit P.** 1991. Pyruvate metabolism of the hyperthermophilic archaebacterium *Pyrococcus furiosus*: acetate formation from acetyl-CoA and ATP synthesis are catalyzed by an acetyl-CoA synthetase (ADP-forming). Arch. Microbiol. **155:**366–377.
14. **Schafer T, Selig M, Schonheit P.** 1993. Acetyl-CoA synthetase (ADP-forming) in archaea, a novel enzyme involved in acetate formation and ATP synthesis. Arch. Microbiol. **159:**72–83. http://dx.doi.org/10.1007/BF00244267.
15. **Labes A, Schonheit P.** 2001. Sugar utilization in the hyperthermophilic, sulfate-reducing archaeon *Archaeoglobus fulgidus* strain 7324: starch degradation to acetate and CO_2 via a modified Embden-Meyerhof pathway and acetyl-CoA synthetase (ADP-forming). Arch. Microbiol. **176:**329–338. http://dx.doi.org/10.1007/s002030100330.
16. **Brasen C, Schonheit P.** 2004. Unusual ADP-forming acetyl-coenzyme A synthetases from the mesophilic halophilic euryarchaeon *Haloarcula marismortui* and from the hyperthermophilic crenarchaeon *Pyrobaculum aerophilum*. Arch. Microbiol. **182:**277–287. http://dx.doi.org/10.1007/s00203-004-0702-4.
17. **Musfeldt M, Selig M, Schonheit P.** 1999. Acetyl coenzyme A synthetase (ADP forming) from the hyperthermophilic archaeon *Pyrococcus furiosus*: identification, cloning, separate expression of the encoding genes, *acdAI* and *acdBI*, in *Escherichia coli*, and *in vitro* reconstitution of the active heterotetrameric enzyme from its recombinant subunits. J. Bacteriol. **181:**5885–5888.
18. **Musfeldt M, Schonheit P.** 2002. Novel type of ADP-forming acetyl coenzyme A synthetase in hyperthermophilic archaea: heterologous expression and characterization of isoenzymes from the sulfate reducer *Archaeoglobus fulgidus* and the methanogen *Methanococcus jannaschii*. J. Bacteriol. **184:**636–644. http://dx.doi.org/10.1128/JB.184.3.636-644.2002.
19. **Awano T, Wilming A, Tomita H, Yokooji Y, Fukui T, Imanaka T, Atomi H.** 2014. Characterization of two members among the five ADP-forming acyl coenzyme A (acyl-CoA) synthetases reveals the presence of a 2-(imidazol-4-yl)acetyl-CoA synthetase in *Thermococcus kodakarensis*. J. Bacteriol. **196:**140–147. http://dx.doi.org/10.1128/JB.00877-13.
20. **Schmidt M, Schonheit P.** 2013. Acetate formation in the photoheterotrophic bacterium *Chloroflexus aurantiacus* involves an archaeal type ADP-forming acetyl-CoA synthetase isoenzyme I. FEMS Microbiol. Lett. **349:**171–179. http://dx.doi.org/10.1111/1574-6968.12312.
21. **Kosaka T, Kato S, Shimoyama T, Ishii S, Abe T, Watanabe K.** 2008. The genome of *Pelotomaculum thermopropionicum* reveals niche-associated evolution in anaerobic microbiota. Genome Res. **18:**442–448. http://dx.doi.org/10.1101/gr.7136508.
22. **McInerney MJ, Rohlin L, Mouttaki H, Kim U, Krupp RS, Rios-Hernandez L, Sieber J, Struchtemeyer CG, Bhattacharyya A, Campbell JW, Gunsalus RP.** 2007. The genome of *Syntrophus aciditrophicus*: life at the thermodynamic limit of microbial growth. Proc. Natl. Acad. Sci. U S A **104:**7600–7605. http://dx.doi.org/10.1073/pnas.0610456104.
23. **Parizzi LP, Grassi MC, Llerena LA, Carazzolle MF, Queiroz VL, Lunardi I, Zeidler AF, Teixeira PJ, Mieczkowski P, Rincones J, Pereira GA.** 2012. The genome sequence of *Propionibacterium acidipropionici* provides insights into its biotechnological and industrial potential. BMC Genomics **13:**562. http://dx.doi.org/10.1186/1471-2164-13-562.
24. **Fraser ME, James MN, Bridger WA, Wolodko WT.** 1999. A detailed structural description of *Escherichia coli* succinyl-CoA synthetase. J. Mol. Biol. **285:**1633–1653. http://dx.doi.org/10.1006/jmbi.1998.2324.
25. **Fraser ME, Joyce MA, Ryan DG, Wolodko WT.** 2002. Two glutamate residues, Glu 208 alpha and Glu 197 beta, are crucial for phosphorylation and dephosphorylation of the active-site histidine residue in succinyl-CoA synthetase. Biochemistry **41:**537–546. http://dx.doi.org/10.1021/bi011518y.
26. **Wolodko WT, Fraser ME, James MN, Bridger WA.** 1994. The crystal structure of succinyl-CoA synthetase from *Escherichia coli* at 2.5-Å resolution. J. Biol. Chem. **269:**10883–10890.
27. **Bridger WA.** 1974. Succinyl-CoA synthetase, 3rd ed, vol 10. Academic Press, New York, NY.
28. **Brasen C, Schmidt M, Grotzinger J, Schonheit P.** 2008. Reaction mechanism and structural model of ADP-forming acetyl-CoA synthetase from the hyperthermophilic archaeon *Pyrococcus furiosus*: evidence for a second active site histidine residue. J. Biol. Chem. **283:**15409–15418. http://dx.doi.org/10.1074/jbc.M710218200.
29. **Diamond LS, Harlow DR, Cunnick CC.** 1978. A new medium for the axenic cultivation of *Entamoeba histolytica* and other *Entamoeba*. Trans. R. Soc. Trop. Med. Hyg. **72:**431–432. http://dx.doi.org/10.1016/0035-9203(78)90144-X.
30. **Bradford MM.** 1976. A rapid and sensitive method for the quantitation of microgram quantities of protein utilizing the principle of protein-dye binding. Anal. Biochem. **72:**248–254. http://dx.doi.org/10.1016/0003-2697(76)90527-3.
31. **Srere PA.** 1963. Citryl-CoA: a substrate for the citrate-cleavage enzyme. Biochim. Biophys. Acta **73:**523–525. http://dx.doi.org/10.1016/0926-6569(63)90146-9.
32. **Bowman CM, Valdez RO, Nishimura JS.** 1976. Acetate kinase from *Veillonella alcalescens*: regulation of enzyme activity by succinate and substrates. J. Biol. Chem. **251:**3117–3121.
33. **Lipmann F, Tuttle LC.** 1945. A specific micromethod for determination of acyl phosphates. J. Biol. Chem. **159:**21–28.
34. **Rose IA, Grunberg-Manago M, Korey SF, Ochoa S.** 1954. Enzymatic phosphorylation of acetate. J. Biol. Chem. **211:**737–756.
35. **Saavedra E, Marin-Hernandez A, Encalada R, Olivos A, Mendoza-Hernandez G, Moreno-Sanchez R.** 2007. Kinetic modeling can describe in vivo glycolysis in *Entamoeba histolytica*. FEBS J. **274:**4922–4940. http://dx.doi.org/10.1111/j.1742-4658.2007.06012.x.
36. **Montalvo FE, Reeves RE, Warren LG.** 1971. Aerobic and anaerobic metabolism in *Entamoeba histolytica*. Exp. Parasitol. **30:**249–256. http://dx.doi.org/10.1016/0014-4894(71)90089-0.
37. **Pineda E, Encalada R, Rodriguez-Zavala JS, Olivos-Garcia A, Moreno-Sanchez R, Saavedra E.** 2010. Pyruvate:ferredoxin oxidoreductase and bifunctional aldehyde-alcohol dehydrogenase are essential for energy metabolism under oxidative stress in *Entamoeba histolytica*. FEBS J. **277:**3382–3395. http://dx.doi.org/10.1111/j.1742-4658.2010.07743.x.
38. **Zuo X, Coombs GH.** 1995. Amino acid consumption by the parasitic, amoeboid protists *Entamoeba histolytica* and *E. invadens*. FEMS Microbiol. Lett. **130:**253–258. http://dx.doi.org/10.1111/j.1574-6968.1995.tb07728.x.
39. **Anderson IJ, Loftus BJ.** 2005. *Entamoeba histolytica*: observations on metabolism based on the genome sequence. Exp. Parasitol. **110:**173–177. http://dx.doi.org/10.1016/j.exppara.2005.03.010.
40. **Clark CG, Alsmark UC, Tazreiter M, Saito-Nakano Y, Ali V, Marion S, Weber C, Mukherjee C, Bruchhaus I, Tannich E, Leippe M, Sicheritz-Ponten T, Foster PG, Samuelson J, Noel CJ, Hirt RP, Embley TM, Gilchrist CA, Mann BJ, Singh U, Ackers JP, Bhattacharya S, Bhattacharya A, Lohia A, Guillen N, Duchene M, Nozaki T, Hall N.** 2007. Structure and content of the *Entamoeba histolytica* genome. Adv. Parasitol. **65:**51–190. http://dx.doi.org/10.1016/S0065-308X(07)65002-7.
41. **Cummings JH, Pomare EW, Branch WJ, Naylor CP, Macfarlane GT.** 1987. Short chain fatty acids in human large intestine, portal, hepatic and venous blood. Gut **28:**1221–1227. http://dx.doi.org/10.1136/gut.28.10.1221.
42. **Fry M, Beesley JE.** 1991. Mitochondria of mammalian *Plasmodium* spp. Parasitology **102:**17–26. http://dx.doi.org/10.1017/S0031182000060297.
43. **van Dooren GG, Stimmler LM, McFadden GI.** 2006. Metabolic maps and functions of the *Plasmodium* mitochondrion. FEMS Microbiol. Rev. **30:**596–630. http://dx.doi.org/10.1111/j.1574-6976.2006.00027.x.